Thermal contact resistance for stationary and moving heat sources in angular contact ball bearings

Sebastian CABEZAS [1],*, **György HEGEDŰS** [1], **Péter BENCS** [2]

[1] Institute of Machine Tools and Mechatronics, University of Miskolc, Miskolc, Hungary
[2] Institute of Energy Engineering and Chemical Machinery, University of Miskolc, Miskolc, Hungary
*Corresponding author: szgtscab@uni-miskolc.hu

Abstract

Sliding friction is a common tribological effect that occurs between the contact surfaces of the inner components (inner race, outer race and balls) of a spindle rolling bearing during operation. This friction generally generates heat, which can affect the performance of the rolling bearing. To date, numerous studies have assumed that the contact surface between the inner components of the bearing is circular and stationary. While this assumption has yielded adequate results, it is not sufficient in the case of angular contact ball bearings, where the contact surfaces are elliptical and could be treated as either stationary or moving heat sources. This paper presents solutions for both, stationary and moving heat sources for elliptical contact surfaces in a spindle rolling bearing. The primary objective is to find the thermal contact resistances which are dependent on the shape of contact, the loads, the rotational speed and the material properties thereof, applying the mathematical expressions developed by Muzychka and Yovanovich. These expressions were used to calculate various thermal resistances, providing results applicable to the analysis of thermal models in spindle rolling elements. Through finite element analysis (FEA) performed in *Ansys Workbench*, the stationary and moving heat sources were compared, finding the heat distribution along the elements of the bearing. The findings herein are suitable for the creation of thermal networks in rolling bearings, which are essential to predict their thermal behaviour.

1. Introduction

Spindle systems are mechanical elements extensively used in different types of machining operations. By and large, the dynamic spindle characteristics are affected by the bearing performance, specifically by its thermal behaviour [1]. Angular contact ball bearings are primarily used in high-speed spindles and other rotary components of machine tools due to their high precision, rigidity and reliability [2]. The internal effects that are produced by the external loads into the bearing, including, sliding, rolling and drag frictional moments, changes in the lubrication viscosity and heat generation [3-4], will lead to an improper functioning of the bearing and subsequently an improper performance of the spindle system. Over the past few years, extensive investigations have been conducted aiming to study the thermal behaviour of ball bearings and the influences in various machining applications.

To mention some relevant investigations regarding the thermal analysis in ball bearings, Li et al. [5] found that heat generation increases when increasing the tilting angle of the bearing outer race, hence demonstrating that geometrical constraints will influence directly the thermal performance of ball bearings in a spindle system. Kim et al. [6] performed a numerical analysis of the frictional torque and the heat generation that occurs by friction in angular contact ball bearings in spindle systems using a 3D half symmetric model by finite element analysis. The results were

compared with experimental measurements, showing good agreement between the calculated and measured results. Liu et al. [7] established a thermal resistance network model for the total spindle system including thermal conduction resistance, thermal contact resistance and the fitted curve of the temperature variation of the cooling system. It could be seen that their proposed thermal model predicts the temperature variation of the main components of the spindle system in comparison with experimental measurements is accurate. Pouly et al. [8] performed an extensive literature survey regarding heat generation and the methods of calculation, which were mainly analysed for bearings under rolling friction and drag moments. Furthermore, a thermal resistance network model was presented, in order to find a thermal model capable of predicting the thermal behaviour of the bearing components.

It is worth mentioning that the determination of the thermal contact resistances is of vast importance in the creation of thermal networks to analyse the heat distribution in rolling bearings of spindle units. Various studies [9-11] have considered this methodology to be a reliable method for predicting the thermal behaviour in bearings of spindle systems.

The aforementioned studies provide a notion of the importance of the applications of thermal analysis in bearings. It is well understood that the researchers have focused their efforts on analysing the internal effects that cause heat generation. Among them, the study and analysis of the frictional moments stand out. However, it is observed that there is no specific approach to calculate the thermal contact resistances resulting from sliding friction between the inner race and balls, as well as the outer race and balls. This friction at the interface of the balls and the inner and outer race of the bearing induces heat and further increases the temperature of the spindle [12]. In angular contact ball bearings, the contact between the surfaces of the outer race, balls and inner race is elliptical, therefore the application of the Hertzian contact theory is of extent importance at calculating the shape and dimensions of the contact areas [13]. The thermal contact resistances produced by sliding friction not only depend on the shape of the contact area but are functions which depend on the applied load, the thermal properties of the elements and the operational speeds. It has been assumed in most studies that the thermal contact between the surfaces of the inner components of a ball bearing is static [14], leading to approximate results in the thermal models. However, this assumption is limited, since moving heat sources are occurring inside the bearing under operation.

This paper presents a study of the thermal resistance models for stationary and moving heat sources for elliptical contact surfaces, which were stated by Muzychka and Yovanovich [15]. The study starts by analysing the forces acting on the angular contact ball bearing during machining operations. The determination of the sliding frictional moment is carried out using the SKF formulation [16], and the heat generation in the inner race, balls and outer race are calculated based on [17]. The study of the thermal resistances of elliptical contact is described in three parts, static heat sources, moving heat sources and a combination of static and moving heat sources. It is worth mentioning that the authors of this paper assume that the reader is acquainted with the Hertzian contact theory. A detailed literature on the analysis of Hertzian contact theory can be found in [18-19]. In this study, the heat flux distribution is analysed for isoflux and parabolic heat distribution. The heat distribution is simulated by *Ansys Workbench Thermal* considering the heat losses as the input variable of the system. The results are tabulated as non-dimensional thermal contact resistances, for stationary, moving and a combination of heat sources, hence, these models can be utilised in the development of thermal models wherein sliding friction within the bearings is of vast importance.

2. Materials and methods

During machining operations, spindle systems are subjected to heavy loads, which are transferred to the components of the high-speed spindle system. Mainly, the angular contact ball bearings absorb these loads, resulting in heat generation due to friction between the inner elements of the bearing. Commonly, the bearings of a spindle system are mounted in a back-to-back arrangement, as shown in Figure 1, to properly accommodate thrust and radial loads [18].

In this study, an angular contact ball bearing model SKF 7203 BEP, which is commonly used in high-speed spindles, is chosen as a representative model. This type of bearing has a contact angle of $\alpha = 40°$, a basic dynamic load rating $C = 10.4$ kN, a basic static load rating $C_0 = 5.5$ kN and a limiting rotational speed $n = 22.000$ rpm. Additionally, due to the applied forces in the bearing, an elliptic contact

surface of the semi-major axis a and semi-minor axis b [13], will be formed between the outer race and ball and the inner race and ball, as shown in Figure 2.
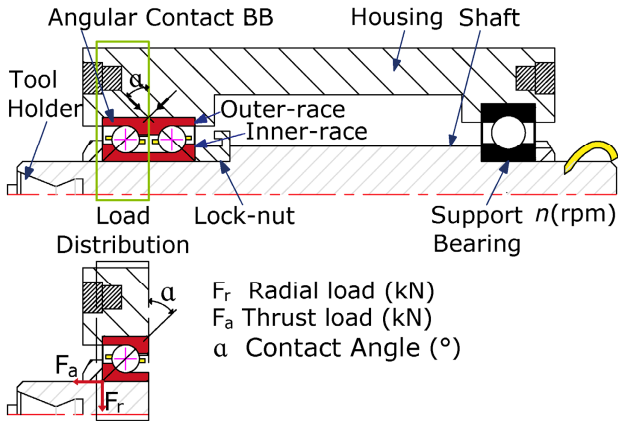

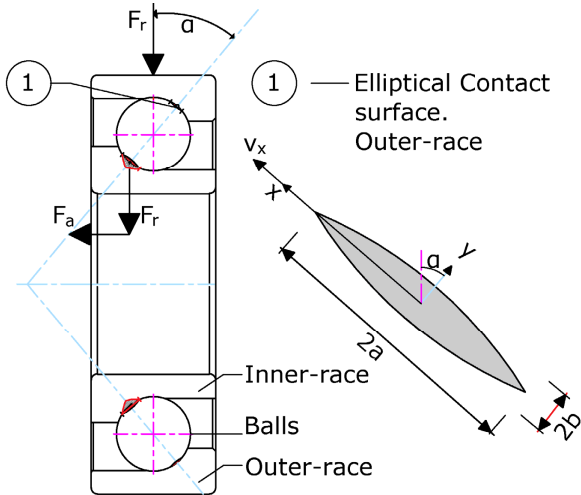**Figure 1.** Schematic view of a spindle system

Figure 2. Elliptical contact surface in an angular contact ball bearing

2.1 Dynamic equivalent radial load, sliding frictional moment and power losses

To determine the sliding frictional moment, the equivalent radial load was calculated using Equation (1) [18].

$$\frac{F_a}{F_r} \leq 0.505\left(\frac{F_a}{C_0}\right)^{0.231} \qquad P_r = F_r$$

$$\frac{F_a}{F_r} > 0.505\left(\frac{F_a}{C_0}\right)^{0.231} \qquad P_r = 0.56F_r + \frac{0.84F_a}{\left(\frac{F_a}{C_0}\right)^{0.24}} \quad (1)$$

The sliding frictional moment given by Equation (2) is calculated using the expression given by the manufacturer of the bearing. A detailed formulation of the sliding frictional moment can be found in [16].

$$M_{sl} = S_1 d_m^{0.26}\left[\left(F_r + S_2 d_m^4 n^2\right)^{4/3} + S_3 F_a^{4/3}\right]\mu_{sl}. \quad (2)$$

The total heat generation, the heat in the balls and the heat in the inner and outer races are calculated by applying Equation (3), based on the heat partition concept [17].

$$\dot{Q}_f = M_{sl}\omega,$$
$$\dot{Q}_{fi} = \dot{Q}_{fo} = 0.25\dot{Q}_f,$$
$$\dot{Q}_{fb} = 0.5\dot{Q}_f. \quad (3)$$

2.2 Stationary and moving heat sources

In this section, a discussion of stationary and moving heat sources is presented. The mathematical formulations to determine the thermal contact resistances are described for stationary, moving and a combination of both. The formulations are based on the investigation performed by Muzychka and Yovanovich [15]. It is worth noting that in their work, study cases related to circular, rectangular and elliptical contact surfaces are presented. However, in the present work, only the elliptical contact is considered, since the real sliding contact in ball bearings is elliptical. To differentiate between a stationary and moving heat source, the Péclet number is calculated and is given by Equation (4).

$$Pe = \frac{v_x l}{\kappa}. \quad (4)$$

Stationary heat sources. Approximate solutions for thermal contact resistances can be obtained by the assumption that the contact surface between the inner components of the bearing is stationary, which means that $Pe_s \to 0$. In this case, two types of heat flux distribution are considered.

The isoflux heat source is given by Equation (5) for average and maximum thermal contact resistance.

$$\overline{R}_s k\sqrt{A} = \frac{16}{3\pi^3}\sqrt{\pi\varepsilon_s}\,K(\varepsilon_s'),$$
$$\hat{R}_s k\sqrt{A} = \frac{2}{\pi^2}\sqrt{\pi\varepsilon_s}\,K(\varepsilon_s'). \quad (5)$$

The parabolic heat source is given by Equation (6) for average and maximum thermal contact resistance.

$$\overline{R}_s k\sqrt{A} = \frac{9}{16\pi}\sqrt{\pi\varepsilon_s}\,K(\varepsilon_s'),$$
$$\hat{R}_s k\sqrt{A} = \frac{3}{4\pi}\sqrt{\pi\varepsilon_s}\,K(\varepsilon_s'). \quad (6)$$

where $\varepsilon_s = b/a$ represents the aspect ratio for stationary contact and $\varepsilon_s' = \sqrt{1 - \varepsilon_s^2}$.

Moving heat sources. In the case of moving heat sources $Pe_m \to \infty$, there are two classifications, non-real and real contacts.

Non-real contact. For parabolic heat distribution, non-real contact has been proposed in the studies of Jaeger [20] and is expressed by Equation (7).

$$\bar{R}_m k \sqrt{A} = 0.323 \left(\frac{a}{b} \right) \frac{1}{\sqrt{Pe_m}},$$

$$\hat{R}_m k \sqrt{A} = 0.589 \left(\frac{a}{b} \right) \frac{1}{\sqrt{Pe_m}}. \quad (7)$$

This approach has been used in some modern research regarding thermal models for ball bearings [2]. As stated by Muzychka and Yovanovich [15], it could lead to appropriate approximations. Nevertheless, it is still considered a non-real contact. The characteristic length $l = a$ in Equation 4), is equal to the semi-major axis a of the elliptical surface.

Real contact. For real contact analysis, a modified Péclet number must be applied, which is a function of the aspect ratio of the ellipse ε_m for moving heat sources, and its characteristic length l is replaced by the square root of the total elliptic contact area $l = \sqrt{A}$. The modified Péclet number $Pe_{\sqrt{A}}^*$ is given by Equation (8).

$$Pe_{\sqrt{A}}^* = (\varepsilon_m)^{1/2} \frac{v_x \sqrt{A}}{\kappa}. \quad (8)$$

For isoflux heat distribution in moving heat sources, the average and maximum thermal contact resistances are given by Equation (9).

$$\bar{R}_m k \sqrt{A} = \frac{0.750}{\sqrt{Pe_{\sqrt{A}}^*}},$$

$$\hat{R}_m k \sqrt{A} = \frac{1.200}{\sqrt{Pe_{\sqrt{A}}^*}}. \quad (9)$$

For parabolic heat distribution in moving heat sources, the average and maximum thermal contact resistances are given by Equation (10).

$$\bar{R}_m k \sqrt{A} = \frac{0.762}{\sqrt{Pe_{\sqrt{A}}^*}},$$

$$\hat{R}_m k \sqrt{A} = \frac{1.390}{\sqrt{Pe_{\sqrt{A}}^*}}. \quad (10)$$

Combined heat sources. When the ball bearings rotate at moderate speeds, it means $0.1 < Pe_m < 10$, it is not possible to assume stationary or moving heat sources. Therefore, a combination of both types of heat sources leads to practical and realistic solutions. As shown in the previous cases, Muzychka and Yovanovich [15] derived formulations for the thermal contact resistance for isoflux and parabolic heat distribution.

For isoflux heat distribution in combined heat sources, the average and maximum thermal contact resistances are given by Equation (11).

$$\bar{R}_c k \sqrt{A} = \frac{0.750}{\sqrt{Pe_{\sqrt{A}}^*} + \dfrac{6.05}{\varepsilon_s K^2(\varepsilon_s')}},$$

$$\hat{R}_c k \sqrt{A} = \frac{1.200}{\sqrt{Pe_{\sqrt{A}}^*} + \dfrac{11.16}{\varepsilon_s K^2(\varepsilon_s')}}. \quad (11)$$

For parabolic heat distribution in combined heat sources, the average and maximum thermal contact resistances are given by Equation (12).

$$\bar{R}_c k \sqrt{A} = \frac{0.762}{\sqrt{Pe_{\sqrt{A}}^*} + \dfrac{5.77}{\varepsilon_s K^2(\varepsilon_s')}},$$

$$\hat{R}_c k \sqrt{A} = \frac{1.390}{\sqrt{Pe_{\sqrt{A}}^*} + \dfrac{10.79}{\varepsilon_s K^2(\varepsilon_s')}}. \quad (12)$$

3. Results

In this section, an application of the stationary and moving heat sources is calculated for an angular contact ball bearing model, SKF 7203 BEP. The maximum applied force P_r was calculated using Equation (1), and it was limited by the maximum value of static load rating C_0, given by the bearing's manufacturer. The sliding frictional moment M_{sl} and the total heat generation $\dot{Q}_f$ were calculated using Equations (2) and (3), respectively, applying an angular velocity within the range of $\omega = 0 - 1050$ rad/s. Figure 3, depicts the sliding friction moment for different load values P_r.
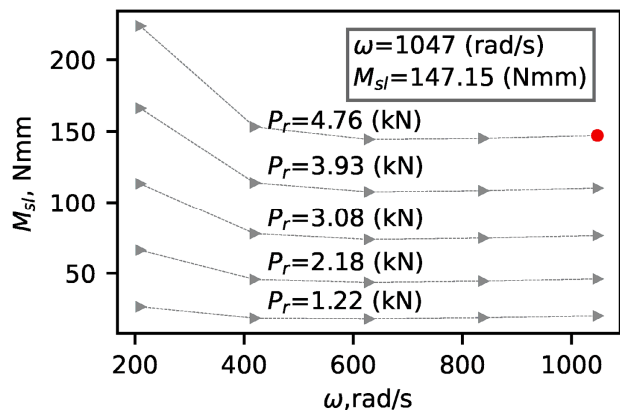

Figure 3. Sliding friction moment vs. angular velocity

Figure 4 depicts the total heat generation $\dot{Q}_f$, that is generated by the sliding frictional moment M_{sl} subjected to the maximum value of equivalent load P_r. Furthermore, the heat distribution along the bearing elements, outer race, balls and inner race are presented.
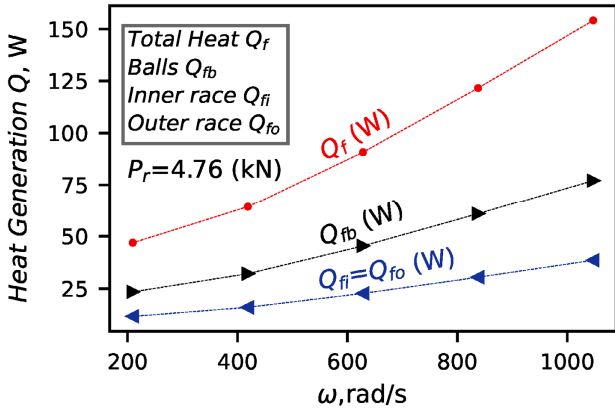

Figure 4. Total heat generation

3.1 Determination of thermal contact resistance

To illustrate, only the thermal contact resistances related to the outer race of the angular contact ball bearing are depicted in Figures 5 to 8. However, the non-dimensional thermal contact resistance values are presented in Tables 1 and 2 for both the inner race and outer race of the angular contact ball bearing.
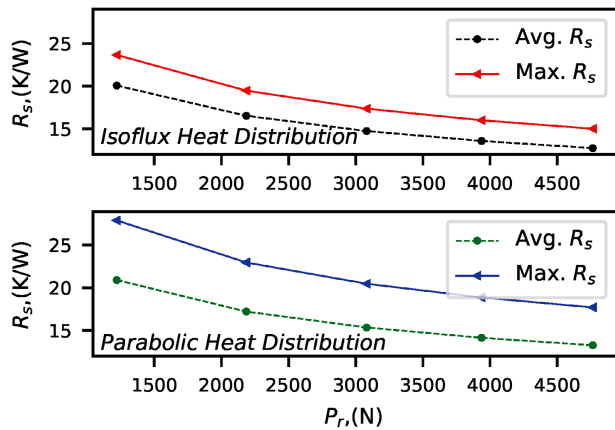

Figure 5. Thermal resistance for stationary heat sources R_s

Thermal contact resistance for stationary heat sources. The thermal contact resistances for stationary heat sources were evaluated using Equation (5) for isoflux and Equation (6) for parabolic heat distribution. The average and maximum values of the thermal contact resistances were determined for a value of the equivalent radial load in the range of $P_r = 0 - 4.8$

kN. Figure 5, depicts the thermal contact resistances of the outer race for isoflux and parabolic heat distribution. It is seen that thermal contact resistance depends on the applied external load, the elliptical contact shape and the thermal properties of the elements.

Thermal contact resistance for moving heat sources. For moving heat sources, the thermal contact resistance depends on the applied external loads, the elliptical contact shape, the thermal properties of the elements and the tangential speed of the races.

Non-real contact moving heat sources were calculated using Equation (7) for parabolic heat distribution. In this case, there is no formulation for isoflux heat distribution. Figure 6 depicts the average and maximum thermal contact resistances of the outer race of the bearing for moving heat sources subjected to the stated maximum applied load P_r.
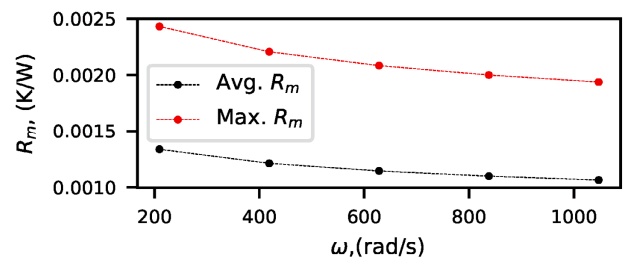

Figure 6. Thermal resistance of non-real contact for moving heat sources R_m

For real contact moving heat sources, the thermal contact resistances for the outer race subjected to the maximum applied load P_r were calculated using Equations (8) and (9) for isoflux and parabolic heat distribution, respectively. The thermal contact resistances are illustrated in Figure 7.
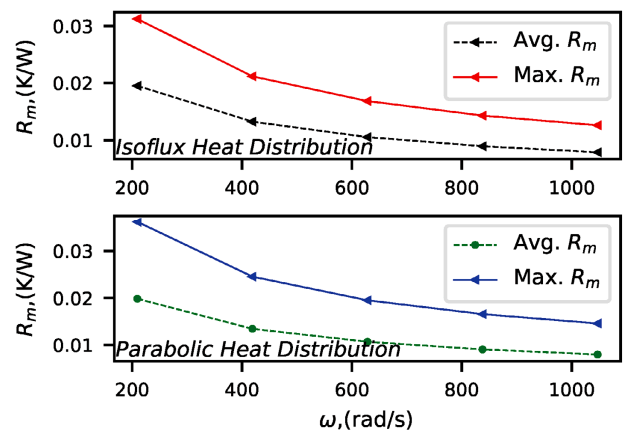

Figure 7. Thermal resistance of real contact for moving heat sources R_m

Thermal contact resistance for combined heat sources. For combined heat sources, Equations (11) and (12) were applied for isoflux and parabolic heat distribution, respectively. Figure 8 depicts the thermal contact resistance of the outer race of the bearing considering the same loads and rotational speeds described in the previous sections.
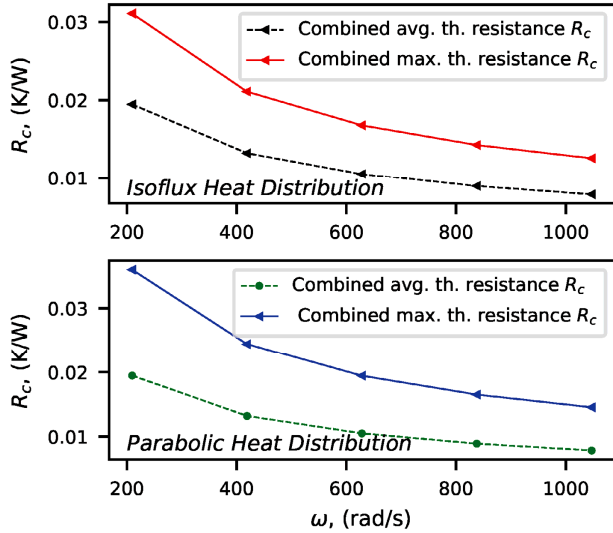

Figure 8. Thermal resistance of real contact for combined heat sources R_c

Table 1 presents the values of the non-dimensional thermal contact resistance for stationary heat sources for the inner and outer race of the angular contact ball bearing. The ball bearing is subjected to an equivalent radial load $P_r = 4.76$ kN.

Table 2 presents the values of the non-dimensional thermal contact resistance for moving and combined heat sources for the inner and outer race of the angular contact ball bearing. The applied force has the same values considered for stationary heat sources. The maximum angular velocity considered for the analysis was equal to $\omega = 0 - 1050$ rad/s.

3.2 FEA simulation

The thermal contact resistances for moving heat sources were evaluated by FEM simulations performed by *Ansys Workbench Thermal*. The analysis was carried out on the outer race of the bearing. The input values for the simulation were the heat generation on the outer race of the bearing $\dot{Q}_{fo}$, the maximum equivalent radial load P_r, the initial temperature of the outer race of the bearing T_{oi} and the effective contact time, which represents the minimum necessary time of contact between two surfaces to act as a thermal contact resistance, given by Equation (13) [15].

Table 1. Non-dimensional thermal contact resistance for stationary heat sources

Heat distribution	Average ($\bar{R}_s k\sqrt{A}$)		Maximum ($\hat{R}_s k\sqrt{A}$)	
	IR	OR	IR	OR
Isoflux	0.0145	0.0127	0.0170	0.0150
Parabolic	0.0151	0.0132	0.0201	0.0176

IR – inner race; OR - outer race

Table 2. Non-dimensional thermal contact resistance for moving heat sources

Non-real contact				
Heat distribution	Average ($\bar{R}_m k\sqrt{A}$)		Maximum ($\hat{R}_m k\sqrt{A}$)	
	IR	OR	IR	OR
Isoflux	–	–	–	–
Parabolic	0.0010	0.0010	0.0019	0.0019
Real contact				
Heat distribution	Average ($\bar{R}_m k\sqrt{A}$)		Maximum ($\hat{R}_m k\sqrt{A}$)	
	IR	OR	IR	OR
Isoflux	0.0008	0.0005	0.0013	0.0009
Parabolic	0.0008	0.0005	0.0015	0.0010
Stationary and moving contact				
Heat distribution	Average ($\bar{R}_c k\sqrt{A}$)		Maximum ($\hat{R}_c k\sqrt{A}$)	
	IR	OR	IR	OR
Isoflux	0.0008	0.0005	0.00013	0.0009
Parabolic	0.0008	0.0005	0.0015	0.0010

IR – inner race; OR – outer race

$$t = \frac{2\sqrt{a^2\left(1 - \frac{y^2}{b^2}\right)}}{v_x}. \tag{13}$$

The temperature variations were calculated by applying the energy equation, given by Equation (14).

$$\dot{Q} = \frac{\Delta T}{R} = \frac{T_f - T_{oi}}{R}. \tag{14}$$

The step end time for the simulation was equal to $t = 0.0001$ s, obtained by Equation (13). The finite elements were selected as tetrahedrons of size 0.001 mm for the volume of the outer race of the bearing. For the contact ellipses, triangular surfaces of size 0.0001 mm were selected. These parameters were considered aiming to obtain factual results. Figure 9 depicts the simulation of the outer race of the bearing under steady-state conditions.
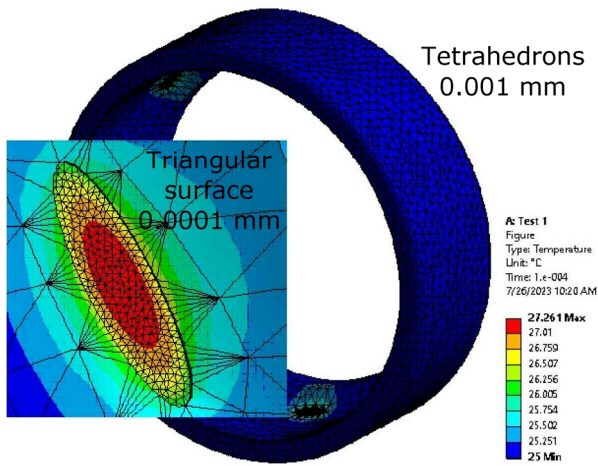
Figure 9. FEA of the outer race of the bearing

The analytical formulations and the FEM simulations were compared for isoflux and parabolic heat distribution and are described in Figure 10.
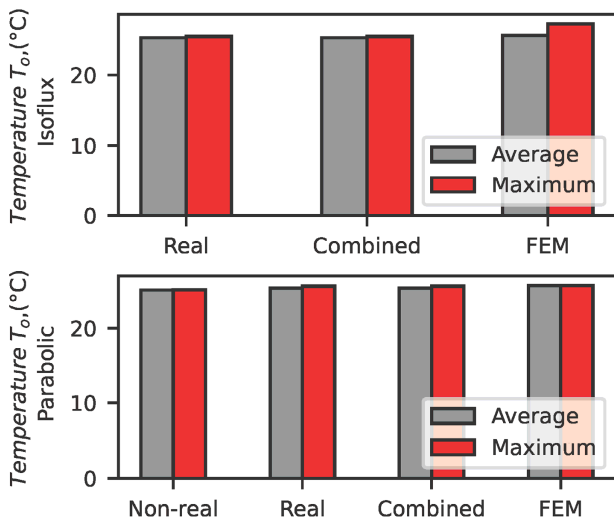

Figure 10. Isoflux and parabolic heat distribution

As depicted in Figure 10, for isoflux distribution, the use of average values of thermal contact resistances results in equal temperature variations for real contact, combined contact and FEM simulation. However, when using maximum values, there will be a temperature difference of approximately $T = 2$ °C.

For parabolic heat distribution, using the average values of thermal contact resistances for real contact, combined contact and FEA simulations leads to a non-representative temperature variation of approximately $T = 0.5$ °C. On the other hand, employing the maximum values of thermal contact resistances shows no significant temperature variations.

4. Conclusions

In this paper, the application of the formulation presented by Muzychka and Yovanovich was

applied in the determination of thermal contact resistances for angular contact ball bearings considering stationary heat sources, moving heat sources and the combination of both. The formulation of the non-dimensional thermal contact resistances for elliptical contact between the inner elements of the bearing was described and the values were tabulated. It could be seen that moving heat sources and combined, on average will have the same non-dimensional values for the inner and outer race of the bearing, respectively. The non-dimensional maximum value of the thermal contact resistances will vary. However, the difference is not representative. It could be seen that reliable results can be obtained by the use of non-real contact for average values. Nevertheless, in the case of maximum values, the differences are more representative. The formulations contained herein can be applied in the creation of thermal networks for spindle systems and their components.

Nomenclature

A	elliptical contact area, mm^2
a	semi-major axis, mm
b	semi-minor axis, mm
C	basic dynamic load rating, kN
C_0	basic static load rating, kN
d_m	bearing mean diameter, mm
F_a	axial load, kN
F_r	radial load, kN
k	thermal conductivity of the bearing material, W/mmK
$K(\varepsilon_s')$	complete elliptic integral of the first kind
l	characteristic length, mm
M_{sl}	sliding friction moment, Nmm
n	rotational speed, rpm
P_r	equivalent radial load, kN
Pe	Péclet number
Pe_m	Péclet number for moving heat sources
Pe_s	Péclet number for stationary heat sources
$Pe_{\sqrt{A}}^*$	modified Péclet number
$\dot{Q}_f$	total heat generation, W
$\dot{Q}_{fb}$	heat generation in the balls, W
$\dot{Q}_{fi}$	heat generation in the inner race, W
$\dot{Q}_{fo}$	heat generation in the outer race, W
R	global thermal resistance, K/W
$\overline{R}_c$	average thermal resistance of the surfaces between the races and balls (combined heat sources), K/W
$\hat{R}_c$	maximum thermal resistance of the surfaces between the races and balls (combined heat sources), K/W

$\bar{R}_{\mathrm{m}}$	average thermal resistance of the surfaces between the races and balls (moving heat sources), K/W
$\hat{R}_{\mathrm{m}}$	maximum thermal resistance of the surfaces between the races and balls (moving heat sources), K/W
$\bar{R}_{\mathrm{s}}$	average thermal resistance of the surfaces between the races and balls (stationary heat sources), K/W
$\hat{R}_{\mathrm{s}}$	maximum thermal resistance of the surfaces between the races and balls (stationary heat sources), K/W
$S_{1/2/3}$	geometry constants of the bearing
t	minimum time of contact to act as a thermal contact resistance, s
T_{f}	final temperature of the outer race, °C
T_{oi}	initial temperature of the outer race, °C
v_x	tangential speed of the inner and outer race of the bearing, mm/s
y	value along the semi-minor axis b, mm
α	contact angle, °
κ	thermal diffusivity, mm^2/s
ε_{s}	aspect ratio for stationary heat sources
ε_{m}	aspect ratio for moving heat sources
μ_{sl}	sliding coefficient of friction

References

[1] D.S. Truong, B.-S. Kim, S.-K. Ro, An analysis of a thermally affected high-speed spindle with angular contact ball bearings, Tribology International, Vol. 157, 2021, Paper 106881, DOI: 10.1016/j.triboint.2021.106881

[2] W. Bian, Z. Wang, J. Yuan, W. Xu, Thermo-mechanical analysis of angular contact ball bearing, Journal of Mechanical Science and Technology, Vol. 30, No. 1, 2016, pp. 297-306, DOI: 10.1007/s12206-015-1233-4

[3] F. Hoffmann, D. Silys, M. Doppelbauer, Transient thermal model for ball bearings in electrical machines, in Proceedings of the International Conference on Electrical Machines (ICEM), 23-26.08.2020, Gothenburg, Sweden, pp. 1018-1024, DOI: 10.1109/ICEM49940.2020.9270718

[4] B. Fang, M. Cheng, T. Gu, D. Ye, An improved thermal performance modeling for high-speed spindle of machine tool based on thermal contact resistance analysis, The International Journal of Advanced Manufacturing Technology, Vol. 120, No. 7-8, 2022, pp. 5259-5268, DOI: 10.1007/s00170-022-09085-4

[5] X. Li, Y. Lv, K. Yan, J. Liu, J. Hong, Study on the influence of thermal characteristics of rolling bearings and spindle resulted in condition of improper assembly, Applied Thermal Engineering, Vol. 114, 2017, pp. 221-233, DOI: 10.1016/j.applthermaleng.2016.11.194

[6] K.-S. Kim, D.-W. Lee, S.-M. Lee, S.-J. Lee, J.-H. Hwang, A numerical approach to determine the frictional torque and temperature of an angular contact ball bearing in a spindle system, International Journal of Precision Engineering and Manufacturing, Vol. 16, No. 1, 2015, pp. 135-142, DOI: 10.1007/s12541-015-0017-1

[7] Y. Liu, Y.-X. Ma, Q.-Y. Meng, X.-C. Xin, S.-S. Ming, Improved thermal resistance network model of motorized spindle system considering temperature variation of cooling system, Advances in Manufacturing, Vol. 6, No. 4, 2018, pp. 384-400, DOI: 10.1007/s40436-018-0239-4

[8] F. Pouly, C. Changenet, F. Ville, P. Velex, B. Damiens, Investigations on the power losses and thermal behaviour of rolling element bearings, Proceedings of the Institution of Mechanical Engineers, Part J: Journal of Engineering Tribology, Vol. 224, No. 9, 2010, pp. 925-933, DOI: 10.1243/13506501JET695

[9] K. Yan, J. Hong, J. Zhang, W. Mi, W. Wu, Thermal-deformation coupling in thermal network for transient analysis of spindle-bearing system, International Journal of Thermal Sciences, Vol. 104, 2016, pp. 1-12, DOI: 10.1016/j.ijthermalsci.2015.12.007

[10] J. Cheng, Z. Zhou, Z. Liu, Y. Zhang, J. Tan, Thermo-mechanical coupling analysis of a high-speed actuating mechanism based on a new thermal contact resistance model, Applied Thermal Engineering, Vol. 140, 2018, pp. 487-497, DOI: 10.1016/j.applthermaleng.2018.05.063

[11] W.-z. Wang, L. Hu, S.-g. Zhang, Z.-q. Zhao, S. Ai, Modeling angular contact ball bearing without raceway control hypothesis, Mechanism and Machine Theory, Vol. 82, 2014, pp. 154-172, DOI: 10.1016/j.mechmachtheory.2014.08.006

[12] J.-H. Huang, V.-T. Than, T.-T. Ngo, C.-C. Wang, An inverse method for estimating heat sources in a high speed spindle, Applied Thermal Engineering, Vol. 105, 2016, pp. 65-76, DOI: 10.1016/j.applthermaleng.2016.05.123

[13] L. Houpert, An engineering approach to Hertzian contact elasticity – Part I, Journal of Tribology, Vol. 123, No. 3, 2001, pp. 582-588, DOI: 10.1115/1.1308043

[14] V.-T. Than, J.H. Huang, Nonlinear thermal effects on high-speed spindle bearings subjected to preload, Tribology International, Vol. 96, 2016, pp. 361-372, DOI: 10.1016/j.triboint.2015.12.029

[15] Y.S. Muzychka, M.M. Yovanovich, Thermal resistance models for non-circular moving heat

sources on a half space, Journal of Heat Transfer, Vol. 123, No. 4, 2001, pp. 624-632, DOI: 10.1115/1.1370516

[16] The SKF model for calculating the frictional moment, available at: https://cdn.skfmediahub.skf.com/api/public/0901d1968065e9e7/pdf_preview_medium/0901d1968065e9e7_pdf_preview_medium.pdf, accessed: 25.09.2023.

[17] J.L. Stein, J.F. Tu, A state-space model for monitoring thermally induced preload in anti-friction spindle bearings of high-speed machine tools, Journal of Dynamic Systems, Measurement, and Control publishes original papers, Vol. 116, No. 3, 1994, pp. 372-386, DOI: 10.1115/1.2899232

[18] H. Nguyen-Schäfer, Computational Design of Rolling Bearings, Springer, Cham, 2016, DOI: 10.1007/978-3-319-27131-6

[19] E. Desnica, A. Ašonja, L. Radovanović, I. Palinkaš, I. Kiss, Selection, dimensioning and maintenance of roller bearings, in D. Blažević, N. Ademović, T. Barić, J. Cumin, E. Desnica (Eds.), 31st International Conference on Organization and Technology of Maintenance (OTO 2022), Springer, Cham, 2023, pp. 133-142, DOI: 10.1007/978-3-031-21429-5_12

[20] J.C. Jaeger, Moving sources of heat and the temperature at sliding contacts, Journal and Proceedings of the Royal Society of New South Wales, Vol. 76, No. 3, 1943, pp. 203-224, DOI: 10.5962/p.360338